ARL-TR-7818 ● SEP 2016

US Army Research Laboratory

Evaluation of Ho:KPb_2Cl_5 as a Diode-Pumpable Mid-IR Laser Material

by Larry D Merkle, Stephen Huerster, and Sudhir B Trivedi

NOTICES

Disclaimers

The findings in this report are not to be construed as an official Department of the Army position unless so designated by other authorized documents.

Citation of manufacturer's or trade names does not constitute an official endorsement or approval of the use thereof.

Destroy this report when it is no longer needed. Do not return it to the originator.

ARL-TR-7818 ● SEP 2016

US Army Research Laboratory

Evaluation of Ho:KPb_2Cl_5 as a Diode-Pumpable Mid-IR Laser Material

by Larry D Merkle
Sensors and Electron Devices Directorate, ARL

Stephen Huerster
Watson School of Engineering, Binghamton University, Binghamton, NY

Sudhir B Trivedi
Brimrose Corporation of America, Glencoe, MD

REPORT DOCUMENTATION PAGE

Form Approved
OMB No. 0704-0188

1. REPORT DATE *(DD-MM-YYYY)*	2. REPORT TYPE	3. DATES COVERED (From - To)
September 2016	Technical Report	

4. TITLE AND SUBTITLE
Evaluation of Ho:KPb2Cl5 as a Diode-Pumpable Mid-IR Laser Material

5a. CONTRACT NUMBER

5b. GRANT NUMBER

5c. PROGRAM ELEMENT NUMBER

6. AUTHOR(S)
Larry D Merkle, Stephen Huerster, and Sudhir B Trivedi

5d. PROJECT NUMBER

5e. TASK NUMBER

5f. WORK UNIT NUMBER

7. PERFORMING ORGANIZATION NAME(S) AND ADDRESS(ES)
US Army Research Laboratory
ATTN: RDRL-SEE-L
2800 Powder Mill Road
Adelphi, MD 20783-1138

8. PERFORMING ORGANIZATION REPORT NUMBER
ARL-TR-7818

9. SPONSORING/MONITORING AGENCY NAME(S) AND ADDRESS(ES)

10. SPONSOR/MONITOR'S ACRONYM(S)

11. SPONSOR/MONITOR'S REPORT NUMBER(S)

12. DISTRIBUTION/AVAILABILITY STATEMENT
Approved for public release; distribution unlimited.

13. SUPPLEMENTARY NOTES

14. ABSTRACT
We have investigated several room-temperature spectroscopic properties of a recently grown crystal of holmium (Ho):KPb_2Cl_5, to evaluate its potential as a diode-pumped mid-IR laser material. We have measured its absorption and fluorescence spectra, and the fluorescence lifetimes of several excited states. These have enabled estimation of the stimulated emission cross section at the 3900-nm peak relevant to laser operation. This crystal shows substantial improvements in lifetime, linewidth, and cross section compared with earlier samples investigated by others, indicative of greatly reduced inhomogeneity. However, very weak absorption in the wavelength range of the most practical laser diodes makes this—and any Ho^{3+}-doped material—very difficult to use as a diode-pumped laser.

15. SUBJECT TERMS
laser material, holmium, fluorescence, lifetime, chloride

16. SECURITY CLASSIFICATION OF:			17. LIMITATION OF ABSTRACT	18. NUMBER OF PAGES	19a. NAME OF RESPONSIBLE PERSON
a. REPORT	b. ABSTRACT	c. THIS PAGE			Larry D Merkle
Unclassified	Unclassified	Unclassified	UU	24	19b. TELEPHONE NUMBER (Include area code) 301-394-0941

Standard Form 298 (Rev. 8/98)
Prescribed by ANSI Std. Z39.18

Contents

List of Figures

List of Tables

1. Introduction

For many applications, solid-state lasers doped with rare-earth ions are more practical than lasers based on gas or liquid gain media, and in many cases, crystalline solids are preferred over glasses. The development of improved laser gain materials thus involves the selection and investigation of favorable combinations of laser gain ion and host crystal. The issues that must be addressed in such development are considerably different for lasers intended to emit at mid-IR wavelengths, such as the 3–5 micron atmospheric window, than for the highly successful lasers that operate around 1 micron.

Many of these issues stem from the fact that longer wavelengths correspond to photons of lower energy, and thus, to smaller energy gaps between the upper and lower laser levels. In solids, one of the major limits on laser efficiency is the decay of the upper laser level without emitting light, due to the simultaneous emission of enough lattice vibrational quanta (phonons) to take the laser ion to the next lower energy level. This multiphonon decay is too weak to be important if many phonons must be emitted at once, but it becomes a major factor if only a few phonons are required to cross the gap between the relevant energy levels. Thus, host crystals whose phonon spectra extend to rather large energies may be fine for shorter-wavelength lasers, but are not useful for 3- to 5-micron lasers. This motivates the investigation of host crystals whose maximum phonon energies are as low as possible.

However, low maximum phonon energies come with a price, since they generally occur in materials with weak interatomic forces, resulting in inferior mechanical properties. Such materials are also often hygroscopic. One class of low-phonon-energy crystal that has gained attention is the alkali-lead-halides, particularly KPb_2Cl_5 (KPC). This material is reported to have low hygroscopicity and has a maximum phonon energy of only 203 cm^{-1}.[1] It has been the subject of several spectroscopic studies involving various rare-earth dopants.[2–8]

The choice of ion introduced into the host crystal to produce laser emission depends on several factors. Clearly, it must have an energy level spacing that can result in emission at the desired laser wavelength, and that state must emit light efficiently. It is also extremely desirable that it absorb light in the wavelength region where laser diodes operate most efficiently, approximately 800–1000 nm. This enables relatively efficient pumping of the upper laser level, contributing to the efficiency of the laser as a whole. The study reported here is motivated by the potential simplicity and efficiency of such diode pumping.

One of the more interesting potential laser ions for emission in the 3- to 5-micron region is holmium (Ho^{3+}). As shown in Fig. 1, it has energy levels separated by energies very appropriate for the goals of this study. The energy spacing between the $^5I_5$ and $^5I_6$ manifolds is about 2500 cm^{-1}, so that in a host with sufficiently weak multiphonon decay, fluorescence can occur at a wavelength of about 4000 nm. The $^5I_5$ manifold lies at an energy corresponding to absorption at about 900 nm, in the wavelength range where laser diodes are particularly efficient. In addition, the potential to pump directly into the upper laser level's manifold should favor high efficiency.

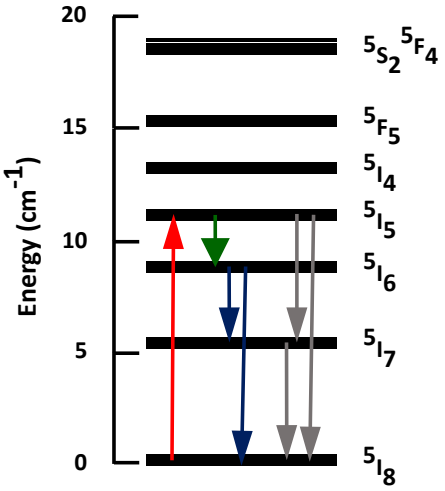

Fig. 1 Schematic energy level diagram of Ho^{3+}. The red arrow indicates the desired absorption transition for populating the intended upper laser level, $^5I_5$. The green arrow is the desired laser transition, and the blue arrows indicate transitions by which the lower laser level can be depopulated, and by which that state's lifetime can be monitored. The gray arrows indicate other fluorescence transitions of use in characterizing the behavior of this ion.

Other groups have investigated some of the properties of Ho:KPC relevant to this study.[9–11] Sardar et al. concentrate on absorption and fluorescence at shorter wavelengths, but use their Judd-Ofelt analysis and evaluation of magnetic dipole contributions to fluorescence to calculate radiative lifetimes for many excited states, including the states that would be the upper and lower laser levels for approximately 4000-nm emission.[9] Oyebola et al. also use Judd-Ofelt analysis, but in addition report fluorescence spectra and lifetimes of various IR transitions, including observation of the $^5I_5 \rightarrow {}^5I_6$ emission at 3900 nm.[10] They use these quantities to calculate the stimulated emission cross section for this peak. Although the spectra reported by Quimby et al. are limited to shorter wavelengths than the 3900-nm band of primary interest in this study, they report both radiative lifetimes of the relevant states, again obtained by Judd-Ofelt analysis, and observed lifetimes.[11]

In this study, we investigate the properties of a more recently grown crystal of Ho:KPC, for which the purification and growth techniques have been improved substantially. This helps us to determine whether the cross sections and lifetimes reported earlier are intrinsic to the material. We also pay particular attention to the prospects for diode pumping this material.

2. Experimental Background

Samples of Ho:KPC were cut from a crystal grown at Brimrose Corporation of America by one of us. After chlorination of the starting materials, the crystal was grown by a modified horizontal Bridgman technique. Details of the crystal growth are given by Brown et al.[12] and the references therein. KPC has a monoclinic crystal structure and thus is optically biaxial.[13] Its nonright angle is 90.05°, so that to the precision available to this group, the principal directions can be treated as orthogonal. We have not used X-ray diffraction or any other means to determine which principal axis is which. The sample used for spectroscopy has a thickness of 0.44 cm.

Absorption spectra were taken using 2 instruments: a Cary 6000i double-arm spectrophotometer for wavelengths 300–1700 nm and a Perkin Elmer Spectrum 2000 Fourier transform IR spectrometer for wavelengths 1430–2500 nm. Fluorescence spectra were taken using a Horiba Fluorolog 3 fluorescence spectrometer with photomultiplier tube (PMT), nitrogen-cooled extended indium gallium arsenide (InGaAs), or nitrogen-cooled indium antimonide photodiode detectors, depending on the desired wavelength range. The output of the photodiodes was measured using a Stanford Research Systems SR830 dual-phase lock-in amplifier. The fluorescence was excited by a tunable Spectra-Physics Tsunami titanium (Ti):sapphire laser, operated in continuous wave mode. Typically, it was tuned to wavelengths in the range of 886–908 nm to excite the $^5I_5$ manifold of Ho^{3+}.

Fluorescence lifetimes were taken using an Instruments SA monochromator, appropriate long-pass filters, and the same PMT or InGaAs photodiode. The signal was captured using a Tektronix TDS 7104 digital oscilloscope. For lifetimes, the fluorescence was excited by the frequency doubled output of a Continuum Surelite Q-switched neodymium (Nd):yttrium aluminum garnet (YAG) laser. The resulting 6-ns pulses at 532 nm were absorbed in the short-wavelength wing of the Ho^{3+} $^5F_4$ manifold's absorption.

All experiments were performed at room temperature.

3. Experimental Data

Using Ti:sapphire laser excitation at 907.44 nm, we have measured the $^5I_5 \rightarrow {}^5I_6$ fluorescence of Ho:KPC, as shown in Fig. 2. Its peak wavelength, approximately 3896 nm, is well within the desired atmospheric window and is well away from any substantial water or carbon dioxide absorption lines. It is this fluorescence that makes this material of interest. The full width at half maximum of this band is 47 nm, much narrower than the 165 nm shown by Oyebola.[10] This suggests that there is considerably less inhomogeneous broadening in this sample with optimized materials preparation and crystal growth parameters.

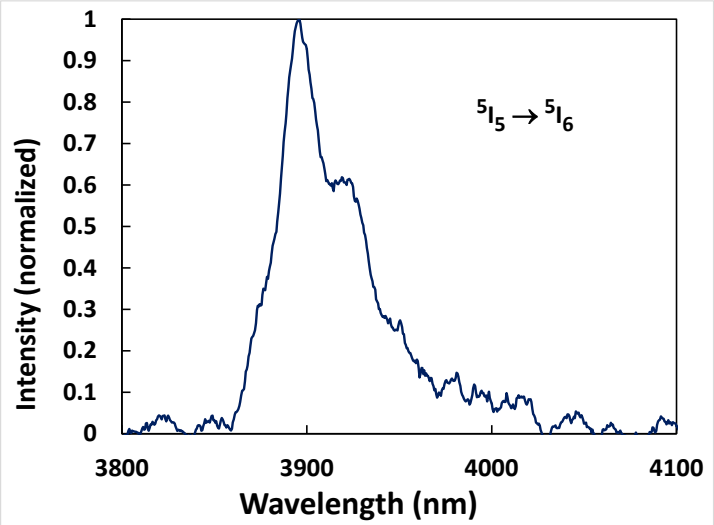

Fig. 2 Mid-IR fluorescence of Ho:KPC

To determine whether this fluorescence is efficient, and investigate potential diode pumping wavelengths, it is useful to know the material's absorption spectra over as wide a wavelength range as possible. This absorption is surveyed in Fig. 3. The spectrophotometer used for wavelengths shorter than 1700 nm is equipped with a polarizer, so the sample was mounted with light propagating along one of the principal axes, and with the other axes horizontal and vertical, within an uncertainty of a few degrees. Spectra were recorded for both horizontally and vertically polarized light. Because it has not been possible to identify which principal axis is which, these spectra are labeled simply as polarizations 1 and 2. The Fourier transform IR spectrometer used for wavelengths longer than 1700 nm lacked this feature, so that spectrum is unpolarized. In these spectra, the transition from the ground-state manifold ($^5I_8$) to the desired upper laser-level manifold ($^5I_5$) appears at about 890–910 nm, and that from the ground state to the desired lower laser-level manifold ($^5I_6$) is at 1150–1200 nm. Both these are weaker than is absorption to some

of the other excited states. The inset of Fig. 3 shows the $^5I_8 \rightarrow {}^5I_5$, the most plausible absorption band for laser diode pumping.

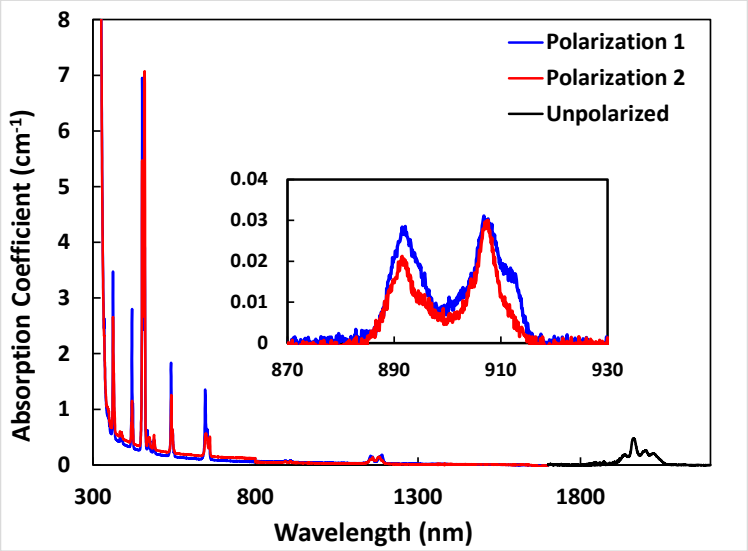

Fig. 3 Absorption spectra of Ho:KPC. For wavelengths shorter than 1700 nm, the spectra are polarized along 2 of the material's 3 principal axes. For longer wavelengths, the spectrum is unpolarized. The inset shows the absorption in the wavelength region of particularly good pump diode lasers.

An idea of the relative efficiencies of population of the upper and lower laser levels can be obtained by measuring fluorescence from those levels following $^5I_5$ excitation. We have measured this fluorescence from Ho:KPC, and for comparison, also from Ho:yttrium oxide (Y_2O_3). (Y_2O_3 is a very robust laser material, although its maximum phonon energy of 591 cm^{-1} is small compared to other oxides, it is much larger than the maximum of 203 cm^{-1} in KPC.[1,14]) The resulting fluorescence spectra are shown in Fig. 4. Although these spectra are not corrected for the wavelength response of the detection system, that response changes gradually enough with wavelength to make the trends clear. In Ho:Y_2O_3, the spectrum is dominated by emission from the $^5I_6$ and $^5I_7$ manifolds. Emission from $^5I_5$ is almost undetectably weak, despite the fact that it is precisely this manifold that is directly excited by the laser. This indicates that in Y_2O_3 the Ho^{3+} $^5I_5$ manifold decays nonradiatively so quickly that almost no fluorescence from that set of states is detectable. Since the most likely nonradiative decay process is the emission of phonons to drop the excited ion from $^5I_5$ to the next lower manifold, $^5I_6$, that manifold is populated efficiently. Both that and the still lower $^5I_7$ emit far more brightly than $^5I_5$, indicating that they do not relax by phonon emission as rapidly as $^5I_5$, and thus live long enough to fluoresce. By contrast, in Ho:KPC the most prominent fluorescence transition in this wavelength range is that from the $^5I_5$. Emission from the $^5I_6$ and $^5I_7$ states is much weaker, indicating that the $^5I_5$ state

decays predominantly radiatively (i.e., by fluorescence,) and that much of that fluorescence is directly to ground state, so that $^5I_6$ and $^5I_7$ are fed to a much smaller degree. This is much more promising for a potential laser material.

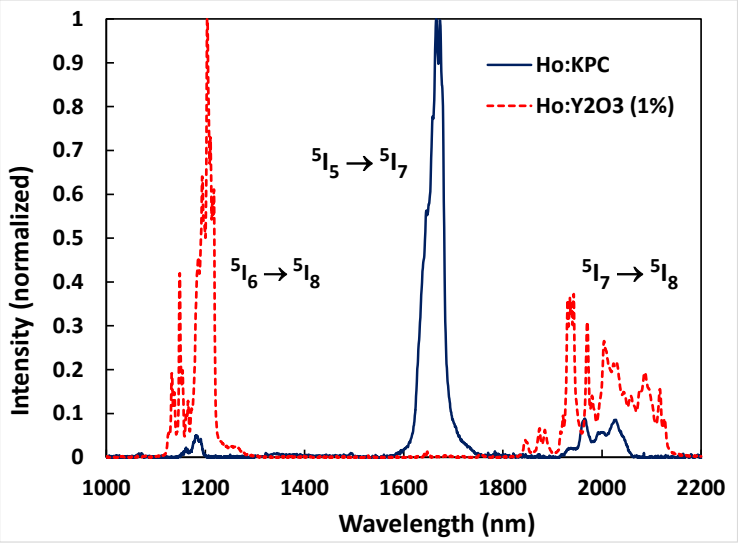

Fig. 4 Near-IR fluorescence of Ho:KPC and Ho:Y_2O_3 upon laser excitation into the $^5I_5$ manifold. The spectra are not corrected for the wavelength dependence of the system sensitivity.

This difference in behavior between Ho:KPC and Ho:Y_2O_3 is consistent with the difference in the 2 hosts' maximum phonon energy. The maximum phonon energy of 591 cm^{-1} in Y_2O_3 means that the energy gap from $^5I_5$ to the next lower manifold can be crossed by the simultaneous emission of only 3 or 4 phonons, whereas the much smaller maximum phonon energy in KPC requires at least 8 phonons to make the same transition. This constitutes a much high-order process and is far less likely to occur, explaining why the $^5I_5$ manifold in Ho:KPC remains excited long enough to fluoresce strongly. The fact that fluorescence from the manifolds $^5I_6$ and $^5I_7$ in Ho:Y_2O_3 is much more detectable than that from $^5I_5$ is consistent with the fact that the energy gaps below these manifolds are significantly larger than the gap below $^5I_5$, requiring more phonons to relax the excited ion across those gaps, and thus making nonradiative decay less rapid.

Knowledge of a laser ion's excited state lifetimes being important for various reasons, we have measured the lifetimes of several excited states of Ho:KPC. For most emission transitions, the observed decay waveforms following pulsed laser excitation are single exponentials, as exemplified in Fig. 5. However, a few of the emission bands exhibit a multi-exponential decay, as exemplified in Fig. 6. We find that these are best fit by a sum of 2 or 3 exponentials, rather than by any more complex function. The possible significance of this difference in behavior for different transitions is considered in Section 5.

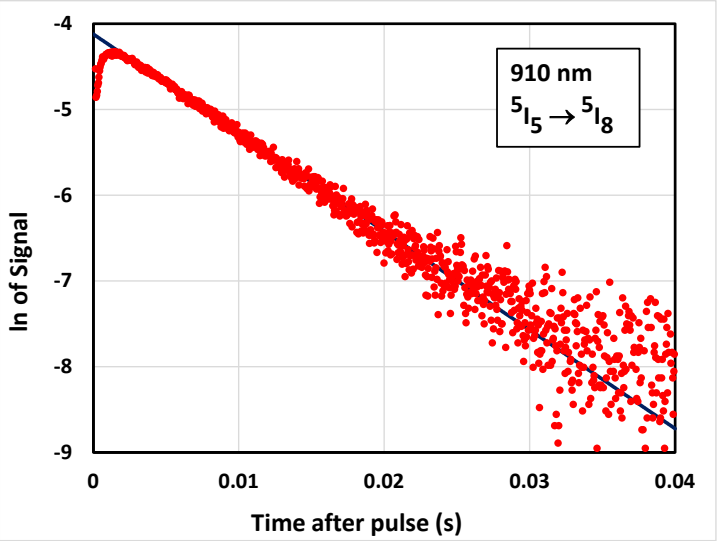

Fig. 5 Decay of Ho:KPC 910-nm fluorescence following pulsed excitation at 532 nm

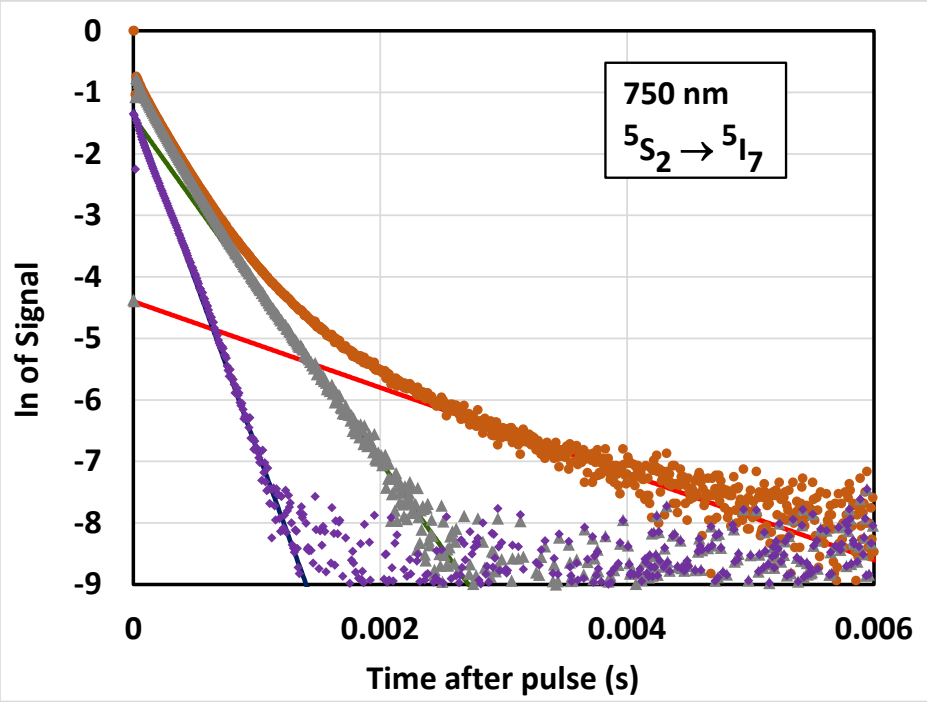

Fig. 6 Decay of Ho:KPC 750-nm fluorescence following pulsed excitation at 532 nm. The decay is fit best by a sum of 3 exponentials. Brown: total signal; Red: fit to tail of decay; Gray: signal minus tail fit; Green: fit to mid-range decay; Violet: signal minus tail and mid-range fits; and Blue: fit to initial decay.

The lifetimes we observed are summarized in Table 1. In some cases, the energies of various manifolds inferred from the absorption data (Fig. 3) are spaced in such a way that a given detection wavelength may correspond to 2 different transitions. In these cases, both are shown. However, consistent assignment of the initial states for emissions observed to have the same lifetime results in unambiguous assignment

of each emission. These transition assignments are listed as "probable", those energetically possible but not giving mutually consistent lifetimes are labeled "possible". The columns showing the lifetimes reported by Quimby et al.[11] and Oyebola et al.[10] are considered in Section 5.

Table 1 Observed fluorescence lifetimes of several excited states of Ho:KPC

Wavelength (nm)	Probable transition	Possible transition	Tail lifetime (ms)	Mid-range lifetime (ms)	Initial lifetime (ms)	Quimby lifetime (ms)	Oyebola lifetime (ms)
650	$^5\mathbf{F_5 \rightarrow {}^5I_8}$	. . .	0.52	. . .	. . .	0.29	. . .
750	$^5\mathbf{S_2 \rightarrow {}^5I_7}$	$^5I_4 \rightarrow {}^5I_8$	1.43	0.38	0.19	0.28	. . .
910	$^5\mathbf{I_5 \rightarrow {}^5I_8}$	. . .	8.70	. . .	. . .	4.90	5.0
1010	$^5\mathbf{S_2 \rightarrow {}^5I_6}$	$^5F_5 \rightarrow {}^5I_7$	1.43	0.38	0.16	0.28	. . .
1180	$^5\mathbf{I_6 \rightarrow {}^5I_8}$	$^5I_4 \rightarrow {}^5I_7$	7.00	. . .	. . .	4.10	4.8
1200	$^5\mathbf{I_4 \rightarrow {}^5I_7}$	. . .	3.30	. . .	0.18	8.30	. . .

4. Data Analysis

We wish to evaluate the potential utility of Ho:KPC as a laser gain medium at mid-IR wavelengths, but the currently available samples do not have sufficiently low loss to lase. As a result, we must rely on spectroscopic data. In such a case, it is extremely useful to determine or estimate the dopant concentration, as an aid to establishing the dopant levels needed for reasonable absorption and calculating cross sections. The Ho concentration in our sample can be estimated with reasonable confidence by comparing our absorption spectra (Fig. 3) with the spectra and concentration reported by Quimby et al.[11] Their Fig. 1a presents polarized absorption data so similar to what we have labeled polarization 2 that their spectrum is clearly due to the same polarization. Comparing these spectra for the 7 strongest and clearest peaks in the 360–660-nm region, and using their reported Ho concentration of 6.9×10^{19} cm^{-3}, it can be inferred that our sample's concentration is 5.3×10^{19} cm^{-3} ($\pm0.34\times10^{19}$).

With this concentration N, the absorption coefficient α, data of Fig. 3 can be converted to absorption cross section σ_a, by the usual relation: $\alpha = N\times\sigma_a$.

Absorption data and dopant concentration can be combined to predict approximate values of other important parameters, using the familiar theory of Judd and Ofelt.[11] Since other groups have done this analysis in recent years,[9–11] we have chosen to use their results, rather than repeat those calculations ourselves. Judd-Ofelt analysis gives approximate predictions of the radiative decay lifetime of any excited manifold and of the branching ratios for emission from any manifold. (For cases in which a particular excited manifold can fluoresce to more than one lower manifold,

branching ratios indicate what fraction of ions in that excited manifold decays radiatively to each lower manifold.) The Judd-Ofelt analysis by Sardar et al.[9] leads to unrealistically long radiative lifetimes for several excited manifolds, suggesting an error that may make other results of theirs unreliable. Thus, we choose to rely on averages of the results from the other 2 groups. The results of interest for present purposes are the predicted radiative lifetime of the $^5I_5$ manifold, 4.6 ms, and the branching ratio for $^5I_5 \rightarrow {}^5I_6$ fluorescence, 0.094.

With these values in hand, the approximate stimulated emission cross section spectrum can be predicted from the observed fluorescence spectrum using the theory of Fuchtbauer and Ladenburg. We use the formulation of this theory developed by Aull and Jenssen,[15] apart from deletion of a mistaken factor of f_j in their Eq. 14. Explicit inclusion of the branching ratio gives the same form used by Oyebola et al.[10]:

$$\sigma_{se}(\lambda) = \frac{\lambda^5 \beta I(\lambda)}{8\pi c n^2 \tau_{rad} \int I(\lambda) \lambda d\lambda} \quad (1)$$

where σ_{se} is the stimulated emission cross section, β is the branching ratio for the transition of interest, I is the fluorescence intensity, c is the speed of light in vacuum, n is the index of refraction in the material, and τ_{rad} is the radiative lifetime of the emitting state. The integral is over the full wavelength range of the fluorescence band. Since our fluorescence spectrum is unpolarized, we use a polarization-average of the published refractive index, 1.94.[16]

Figure 7 shows the resulting stimulated emission spectrum for 2 choices of τ_{rad}: the value predicted by Judd-Ofelt analysis noted previously and our observed $^5I_5$ fluorescence lifetime. The justification for the latter choice is as follows. The observed lifetime, 8.7 ms, is considerably longer than the Judd-Ofelt prediction. Combined with the small maximum phonon energy, this makes it implausible that nonradiative decay is shortening the observed lifetime significantly, relative to the radiative value. Regarding why the observed lifetime would actually be longer than the Judd-Ofelt value, it must be kept in mind that the Judd-Ofelt theory is based on several approximations, so that its results are always approximate. In addition, the only mechanism that could make the observed lifetime longer than the radiative lifetime is reabsorption, a process in which an emitted photon is absorbed by an unexcited ion so that the newly excited ion can now fluoresce in turn. However, for emission from the $^5I_5$ manifold this would require absorption at or near 900 nm, and the inset of Fig. 3 shows that the absorption in this wavelength range is quite weak for any sample thickness less than several centimeters. With a sample thickness of only 0.44 cm, the reabsorption is estimated to be less than 1%, which would stretch the observed lifetime by only about that percentage. Thus, the most plausible

interpretation is that the observed $^5I_5$ lifetime is approximately the radiative lifetime.

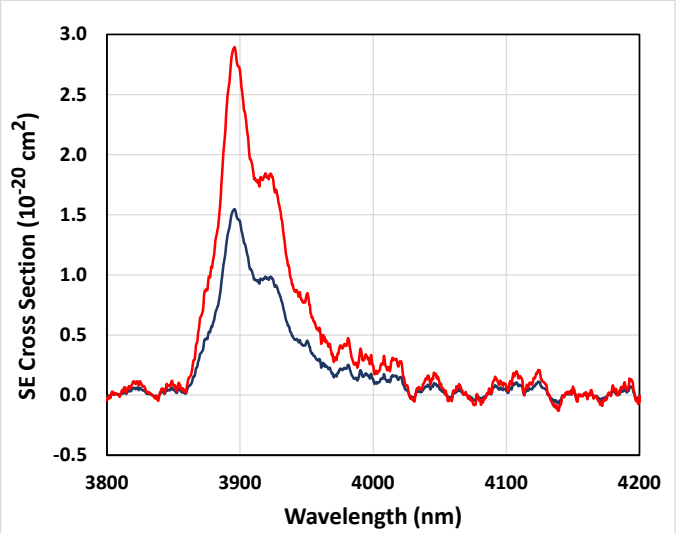

Fig. 7 Mid-IR ($^5I_5 \rightarrow {}^5I_6$) stimulated emission spectrum of Ho:KPC. Red: calculated using the average of the Judd-Ofelt radiative lifetime predictions of references[10,11] and blue: calculated using our observed fluorescence lifetime.

5. Discussion

The Ho:KPC crystal investigated in this work exhibits evidence of significant improvement over the crystals studied a few years ago by other groups. Perhaps most striking is that the peak stimulated emission cross section at about 3900 nm is found in this study to be 1.5 to 2.9×10^{-20} cm^2, depending on which lifetime is closer to radiative, whereas it was previously reported to be approximately 0.6×10^{-20} cm^2.[10] The principal reason for this difference is the width of the stimulated emission band, observed to be only 48 nm full width at half maximum in this study, but reported to be about 165 nm by Oyebola et al. This very probably indicates that the improvements in material preparation and crystal growth embodied in our crystal have achieved a substantial reduction in inhomogeneous broadening. With less inhomogeneous broadening, the total transition strength between 2 manifolds is not spread so widely over wavelength, resulting in higher strength at the peak of the band.

Another substantial difference between the material investigated here and that studied by others lies in its fluorescence lifetimes. Almost all the manifolds measured exhibit significantly longer lifetimes in the current study than those reported by Oyebola et al. and Quimby et al., as shown in Table 1.[10,11] The one exception is the $^5I_4$ manifold, for which we observe a complex decay with a tail lifetime of 3.3 ms, whereas Quimby reports 8.3 ms. The reason for this is not clear.

There are 3 possible explanations for the longer lifetimes we observe for most excited states in this new material: radiative reabsorption in our measurements, increased radiative decay rates in the older material, and increased nonradiative decay rates in that material. Of these, the third is the most plausible. Regarding reabsorption, only the $^5S_2$ emission to the ground state is at a wavelength encountering significant absorption, and for the sample size used, even that could only stretch the lifetime by 10%–15%. This is far smaller than the difference between either the tail or the mid-range lifetimes observed in this study and the lifetime reported by Quimby. Regarding increased radiative decay rates in the earlier material, this could occur if poorer crystal quality distorted the Pb sites, in which rare-earth dopants are thought to reside, so as to break down symmetry-based selection rules. However, even in the perfect crystal, these sites do not have high symmetry,[13] so it is unlikely that additional distortion would make a large change in the decay rate. It is more plausible that poor crystal quality creates defects to which dopants can transfer their energy radiationlessly, thus shortening lifetimes.

Although most of the fluorescence decays we observe are single exponentials, the decays of $^5S_2$ and $^5I_4$ are more complex. It may be significant that of the excited states whose decays could be monitored in the study, these are the 2 that are most susceptible to decay by cross-relaxation. This is because the energy difference between the $^5S_2$ and $^5I_4$ manifolds overlaps that between $^5I_7$ and $^5I_8$, as does that between $^5I_4$ and $^5I_6$. Thus, it is very possible that the faster components of the $^5S_2$ and $^5I_4$ are due to cross-relaxation between Ho^{3+} ions that sit sufficiently close together, as illustrated in Fig. 8. The slower tail components of those decays would be due to the decay of ions too widely separated from each other for cross-relaxation to be significant.

Note that Quimby et al. did not report any such complex decays, instead stating that all waveforms were single exponentials to within experimental uncertainty.[11] If the complex decays we observe for $^5S_2$ and $^5I_4$ are due to cross-relaxation or any other form of ion-ion interaction, it must be that a significant fraction of the dopant ions sit closer together than in the samples investigated by that group. This suggests that, although the quality of the newer crystal used in our study appears to be better overall, it may have more pairs or clusters of Ho^{3+} ions than did the older samples.

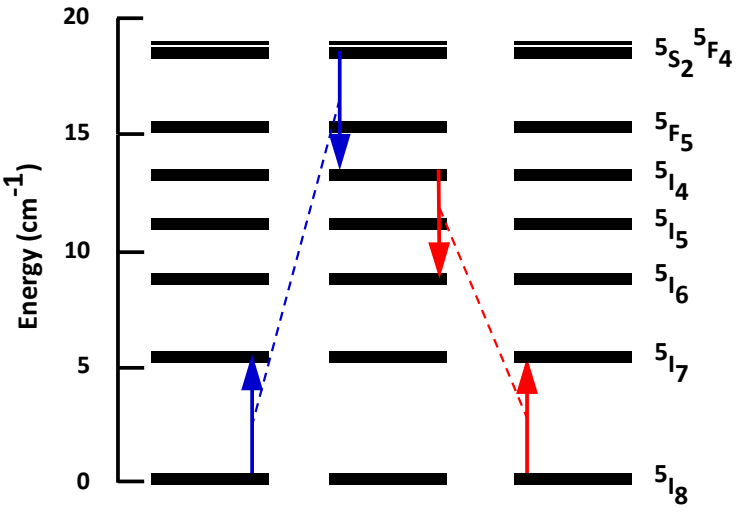

Fig. 8 The 2 energetically favored cross-relaxation processes in Ho:KPC. Blue: a process involving 2 Ho^{3+} ions with initial states $^5S_2$ and $^5I_8$, and final states $^5I_4$ and $^5I_7$. Red: a process involving 2 Ho^{3+} ions with initial states $^5I_4$ and $^5I_8$, and final states $^5I_6$ and $^5I_7$.

The lifetime of the $^5I_5$ manifold, the upper laser level for any approximately 4-micron laser based on Ho^{3+}, is attractively long in Ho:KPC. For pulsed laser operation, this 8.7-ms lifetime would allow pumping by very long (multi-millisecond) diode laser pulses, thus achieving large pulse energies from relatively low-power pumps. For continuous wave operation, standard treatments of lasers show that the gain is proportional to the product of the stimulated emission cross and the upper state lifetime. In the present case, this product is a quite favorable 1.3 to 2.5×10^{-22} cm^2-s. For comparison, this product for the highly successful Nd:YAG laser at 1064 nm is 0.6×10^{-22} cm^2-s.[17]

The lifetime of the $^5I_6$ manifold, the lower laser level, 7.0 ms, is of more concern. It is shorter than the upper laser-level lifetime, so that a laser operating on the $^5I_5 \rightarrow {}^5I_6$ transition would not be "bottlenecked" by the lower-level lifetime, but it is long enough to limit the rate at which the lower laser level can depopulate. There are possible methods to shorten this lifetime. One would be to co-dope the crystal with Tb^{3+}, that is, to use Ho,Tb:KPC as the laser gain medium. The several closely spaced manifolds of terbium (Tb^{3+}) lie lower in energy than the Ho^{3+} $^5I_6$ manifold, so that state of Ho^{3+} may be depopulated by energy transfer to Tb^{3+}. However, the energy difference between Ho^{3+} $^5I_6$ and the highest of relevant states of Tb^{3+} is rather large, approximately 2800 cm^{-1}. Thus, energy transfer would probably be less efficient than has been reported for the pairing of Tb^{3+} with a different potential laser ion, thulium (Tm^{3+}), for which the energy mismatch is far smaller.[6] Another possibility for depopulating the $^5I_6$ would be by simultaneously lasing Ho:KPC on 2 transitions in cascade: $I_5 \rightarrow {}^5I_6$ to give the desired 3900-nm output and $^5I_6 \rightarrow {}^5I_8$

to depopulate $^5I_6$. A similar scheme has recently been demonstrated for lasing Er:Y_2O_3.[18]

The largest impediment to the use of Ho:KPC as a diode-pumped, mid-IR laser is its very weak absorption in the most favorable wavelength region for laser diode pumping. Options for improving this are quite limited. Stronger absorption at longer wavelengths cannot be used, as those bands populate manifolds below the desired upper laser level. The next-higher manifold, $^5I_4$, has even weaker absorption —too weak to be discernable in Fig. 3. There is much stronger absorption into the $^5F_5$ at about 640–660 nm. With a peak absorption coefficient of about 1.3 cm^{-1} for the concentration currently available, a gain medium thickness of 1 or 2 cm would absorb most of the pump power. The drawback is that laser diodes in this wavelength region are not well developed for high output power.

6. Conclusion

We have investigated several spectroscopic properties of Ho:KPb_2Cl_5 to consider its applicability as a diode-pumped, mid-IR laser. This has included comparing properties of a crystal grown using improved techniques and starting materials with those of older samples studied by other groups. In this new material, we observed significantly improved properties, especially a longer upper laser-level lifetime, narrower spectral features, and a significantly higher stimulated emission cross section at the 3900-nm peak. This emission band of Ho^{3+} does not suffer from ground-state absorption, though the long lifetime of the lower laser level may require additional measures to maintain a good population inversion. The one particularly difficult problem to overcome is one that is common to Ho^{3+} in any host familiar to us: the extremely weak absorption of the $^5I_5$ manifold, which requires either unrealistically long path lengths for efficient pump absorption or a switch of pump wavelength to a region where laser diodes are not as well developed for high power use. This may deter laser development of any Ho^{3+}-doped, solid-state material for mid-IR use, including KPC.

7. References

1. Isaenko L, Yelisseyev A, Tkachuk A, Ivanova S. New monocrystals with low phonon energy for mid-IR lasers. In: Mid-infrared coherent sources and applications. Ebrahim-Zadeh M, Sorokina IT, editors. Berlin (Germany): Springer; 2008. p. 3–65.

2. Bowman SR, Searles SK, Ganem J, Schmidt P. Further investigations of potential 4 μm laser materials. In: OSA TOPS vol. 26 advanced solid-state lasers. Fejer MM, Injeyan H, Keller U, editors. Washington (DC): Optical Society of America; 1999. p. 487–490.

3. Nostrand MC, Page RH, Payne SA, Isaenko LI, Yelisseyev AP. Optical properties of Dy^{3+}- and Nd^{3+}-doped KPb_2Cl_5. J Opt Soc Am B. 2001;18(3):264–276.

4. Basiev TT, Orlovskii YuV, Galagan BI, Doroshenko ME, Vorob'ev IN, Dmitruk LN, Papashvili AG, Skvortsov VN, Konyushki VA, Pukhon KK, Ermakov GA, Osiko VV, Prokhorov AM, Smith S. Evaluation of rare-earth doped crystals and glasses for 4-5-μm lasing. Laser Phys. 2002;12(5):859–877.

5. Ferrier A, Velazquez M, Doualan J-L, Moncorge R. Midinfrared luminescence properties and laser potentials of Pr^{3+} Doped KPb_2Cl_5 and $CsCdBr_3$. J Appl Phys. 2008;104:123513.

6. Lichkova NV, Zagorodnev VN, Butvina LN, Okhrimchuk AG, Shestakov AV. Preparation and optical properties of tare-earth-activated alkali metal lead chlorides. Inorg Mater. 2006;42(1):81–88.

7. Tkachuk AM, Ivanova SE, Joubert M-F, Guyot Y, Isaenko LI, Gapontsev VP. Upconversion processes in Er^{3+}:KPb_2Cl_5 laser crystals. J Lumin. 2007;125:271–278.

8. Howse D, Logie M, Bluiett AG, O'Connor S, Condon NJ, Ganem J, Bowman SR. Optically-pumped mid-IR phosphor using Tm^{3+}-sensitized Pr^{3+}-doped KPb_2Cl_5. J Opt Soc Am B. 2010;27(11):2384–2392.

9. Sardar DK, Chandrasekharan SR, Nash KL, Gruber JB, Burger A, Ro UN. Intensity analysis and crystal-field modeling of Ho^{3+} in KPb_2Cl_5 host. J Appl Phys. 2008;103:093112.

10. Oyebola O, Hommerich U, Brown E, Trivedi SB, Bluiett AG, Zavada JM. Growth and optical spectroscopy of Ho-doped KPb_2Cl_5 for infrared solid-state lasers. J Cryst Growth 2010;312:1154–1156.

11. Quimby RS, Condon NJ, O'Connor SP, Bowman SR. Excited state dynamics in Ho:KPb_2Cl_5. Opt Mater. 2012;34:1603–1609.

12. Brown EE, Hommerich U, Kumi-Barimah E, Bluiett A, Trivedi SB. Comparative spectroscopic studies of Ho:KPb_2Cl_5, Ho:KPb_2Br_5, and Ho:YAG for 2 μm laser cooling applications. Proc SPIE. 2015;9380:93800O-1-7.

13. Merkulov AA, Isaenko LI, Pashkov VM, Mazur VG, Virovets AV, Naumov DYu. Crystal structure of KPb_2Cl_5 and KPb_2Br_5. J Struct Chem. 2005;46(1):103–108.

14. Repelin Y, Proust C, Husson E, Beny JM. Vibrational spectroscopy of the C-form of yttrium sesquioxide. J Sol St Chem. 1995;118:163–169.

15. Aull BF, Jenssen HP. Vibronic interactions in Nd:YAG resulting in nonreciprocity of absorption and stimulated emission cross sections. IEEE J Quantum Electron. 1982;QE-18(5):925–930.

16. Condon NJ, O'Connor S, Bowman SR. Growth and characterization of single-crystal Er^{3+}:KPb_2Cl_5 as a mid-infrared laser material. J Crystal Growth. 2006;291:472–478.

17. Koechner W. Solid-state laser engineering. 5th ed. Berlin (Germany): Springer; 2008. p. 48.

18. Sanamyan T. Diode pumped cascade Er:Y_2O_3 laser. Laser Phys Lett. 2015;12:125804.

List of Symbols, Abbreviations, and Acronyms

Ho	holmium
InGaAs	indium gallium arsenide
IR	infrared
KPb_2Cl_5	KPC
Nd	neodymium
PMT	photomultiplier tube
Tb^{3+}	terbium
Tm^{3+}	thulium
Y_2O_3	yttrium oxide
YAG	yttrium aluminum garnet

1 (PDF) DEFENSE TECHNICAL INFORMATION CTR DTIC OCA

2 (PDF) DIRECTOR US ARMY RESEARCH LAB RDRL CIO LL IMAL HRA MAIL & RECORDS MGMT

1 (PDF) GOVT PRNTG OFC A MALHOTRA

5 (PDF) DIRECTOR US ARMY RESEARCH LAB RDRL SEE L L MERKLE M DUBINSKIY A MOTT T SANAMYAN Z FLEISCHMAN

INTENTIONALLY LEFT BLANK.